

ADAPTIVE STRATEGIES FOR MULTIPLE TRANSMIT-RECEIVE ANTENNA WIRELESS COMMUNICATION SYSTEMS

F.R.P. Cavalcanti and J.C.M. Mota

Dep. Eng. Elétrica, Universidade Federal do Ceará
CP 6001, CEP 60451970, Fortaleza-CE, Brasil
e-mails: rod@dee.ufc, mota@dee.ufc

ABSTRACT

In this paper we investigate the effect of different adaptive strategies on the bit error rate of a multiple transmit-receive antenna wireless link. The implementation on the receiver side is based on a linear adaptive antenna array that performs interference cancellation. Aspects such as data block length, training overhead and type of adaptive algorithm updating are discussed. The achievable spectral efficiencies with these strategies are very high as compared to conventional single input-single output wireless links.

1. INTRODUCTION

Recently, very high spectral efficiencies have been demonstrated to be practical on the wireless channel when both the transmitter and receiver employ multiple antennas (e.g. [1-3]). Most works on this subject assume the availability of perfect channel state information at the receiver or at both transmitter and receiver.

In this paper we consider the antenna array receiver operating as a linear interference cancellation array. For such, we employ the direct matrix inversion adaptive algorithm with different updating strategies. We then describe the effect of these different adaptation strategies in the bit error rate (BER) of the recovered data stream. We also test the system sensitivity to other parameters such as data block length and the amount of training overhead.

2. SYSTEM DESCRIPTION

A high-level system block diagram is shown in Fig. 1. Multilevel PSK or QAM transmitters (1 to N) operate co-channel at the same symbol rate $1/T$ with synchronized symbol timing. The transmission procedure is simple: transmission data is split into N sub-streams and independently transmitted by transmitters 1 to N . The total transmitted power is fixed and normalized to 1. For simplicity we assume all transmitters operating with the same type of modulation.

In the receiver side, an antenna array composed of $M \geq N$ antennas is connected to N sets of M -vectors $\mathbf{w}_1 \dots \mathbf{w}_N$ (weight vectors), which aim the recovery of each of the sub-streams. After detection, the sub-streams are re-ordered and converted to the serial unique stream that constitutes the estimated transmitted data.

The wireless channel is modeled as possessing rich scattering such that the $N \times M$ channel matrix \mathbf{H} is composed of independent entries. Flat and slow Rayleigh fading is assumed as model for each entry h_{ij} of \mathbf{H} , i.e., the complex gain from antenna i to antenna j , $1 \leq i \leq N$, $1 \leq j \leq M$. Relative propagation delays among different sub-streams are assumed negligible when compared to the symbol period.

By assuming symbol-rate sampling and perfect synchronization among all receivers, we have a discrete-time model for the received signal M -vector:

$$\mathbf{x}(n) = \sqrt{\frac{\mathbf{r}}{M}} \mathbf{a}(n) \mathbf{H} + \mathbf{v}(n) \quad (1)$$

where $\mathbf{a}(n) = [a_1(n) \dots a_N(n)]^T$ is the N -vector of transmitted symbols by each transmitting antenna, $E\{|a_i(n)|^2\} = 1$, $i=1, \dots, N$; $\mathbf{v}(n)$ is a vector of temporally and spatially white gaussian unit variance noise samples across the antenna array. Finally, \mathbf{r} is the signal to noise ratio (SNR) per receive antenna.

The transmission is organized in burst of L symbols per transmitting antenna. The fading in the channel is assumed to be quasi-static, that is, matrix \mathbf{H} is constant over the transmission of a set of M parallel bursts (one per transmitting antenna) but it is independent between the transmission of each set of bursts.

3. ADAPTIVE STRATEGIES

The antenna array at the receiver operates as a linear interference cancellation array. The signal output by each weight vector is given by:

$$y_i(n) = \mathbf{w}_i^H(n) \mathbf{x}(n), \quad i=1 \dots N \quad (2)$$

where superscript H indicate transpose conjugate. The optimal weight vector in the minimum mean squared error (MMSE) sense for each spatial filter is given by [4]:

$$\mathbf{w}_{i,op} = \mathbf{R}^{-1} \mathbf{p}_i, \quad i=1 \dots N \quad (3)$$

where $\mathbf{R} = E\{\mathbf{x}(n) \mathbf{x}^H(n)\}$ and $\mathbf{p}_i = E\{a_i^*(n) \mathbf{x}(n)\}$. In practice, we need to make available part of the transmitted signal to the receiver so we can compute \mathbf{w}_i in real-time. For such, a training sequence is embedded in each burst. This reference signal is then used for weight acquisition by means of an adaptive algorithm. Typical training overheads range from 10% to 30% of the burst length.

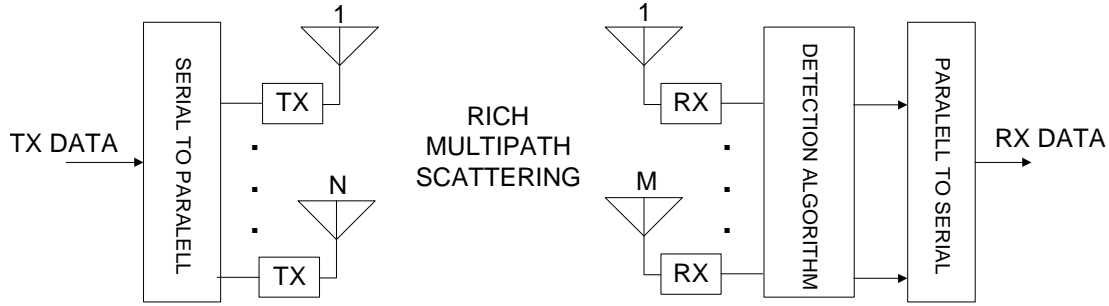


Fig.1 - Multiple Transmit-Receive Antenna Communications Architecture

The direct matrix inversion (DMI) algorithm is one of the most conceptually simple adaptive algorithms. It carries out (3) directly by using real-time averages of \mathbf{R} and \mathbf{p}_i :

$$\hat{\mathbf{R}}(n) = \mu \hat{\mathbf{R}}(n-1) + (1-\mu)\mathbf{x}(n)\mathbf{x}^H(n) \quad (4.a)$$

$$\hat{\mathbf{p}}_i(n) = \mu \hat{\mathbf{p}}_i(n-1) + (1-\mu)a_i^*(n)\mathbf{x}(n) \quad (4.b)$$

$$\mathbf{w}_i(n) = \hat{\mathbf{R}}^{-1}(n) \hat{\mathbf{p}}_i(n) \quad (4.c)$$

where μ is an averaging factor that controls rate of adaptation and quality of the averages.

Besides the training period, the algorithm can also be driven by its own decisions, in the well-known decision-directed mode (DD). This mode is feasible after the training period when reliable decisions can be expected.

Now, consider the following adaptation strategies for the weight vectors $\mathbf{w}_i(n)$, $i=1, \dots, N$:

- a. Training only: the weight vectors are updated during the training period; after this the weight vectors are frozen in order to detect useful data
- b. Training period followed by decision-direction (Training+DD): after the training period the algorithm enters a DD mode while detecting useful data
- c. Reprocessing of useful data (Reprocess): after following step b. we frozen the weight vectors and filter the useful data again.

Clearly, from strategy a. to strategy c. the amount of information used in the computation of the weight vectors increases and so the quality of the output data stream. On the other hand increased computational cost is demanded.

We will try to illustrate the tradeoffs among these adaptation strategies based on their impact on the bit error rate of the recovered data stream.

To finalize this section, we discuss shortly about the choice of the DMI averaging factor μ in (4).

The averaging in the DMI algorithm is based on a rectangular window that can be written as:

$$\hat{z}(n+1) = \frac{1}{n+1} \sum_{i=1}^{n+1} z(i) \quad (5)$$

where $z(n)$ is a generic quantity to be estimated. It is straightforward to show that

$$\hat{z}(n+1) = \frac{n}{n+1} \hat{z}(n) + \frac{1}{n+1} z(n+1) \quad (6)$$

which can be understood as (4.a) or (4.b) when $\mathbf{m} = \frac{n}{n+1}$ and

$z(n)$ fits to the desired quantity. Equation (6) indicates that the averaging factor μ should be a time-varying one, actually. For simplicity we would like to set $\mathbf{m}(n)$ constant. In this case, once the burst length L is set, we can choose $\mathbf{m}(n)$ to match the size of the averaging window, that is $\mathbf{m}(n) = \mu = \frac{L}{L+1}$. Subsequent

simulation results follow this rule for choosing μ . This choice is based on the slow fading assumption during each burst. If the channel exhibits significant time-variation during a single burst, then the choice of μ should be based on an estimate of the coherence time of the channel.

4. PERFORMANCE RESULTS

We tested two array configurations: $N=4, M=8$ (4-8 system) and $N=8, M=12$ (8-12 system). The modulation in each sub-stream is QPSK. The algorithm is run over data blocks of length $L=100$ or $L=500$ symbols. For each case, training overheads of 10%, 20% and 30% of the burst length are employed. The signal to noise ratio per receive antenna is varied in the range 5 to 15 dB in steps of 1 dB. BER performances as a function of the SNR per receive antenna is an average over the transmission of 10^3 data bursts per transmit antenna.

Figs. 2 to 13 show the BER x SNR performance with varying burst length, training overhead, updating strategy and $N-M$ architecture. We also include the limiting optimal MMSE performance for reference.

Figs. 14 to 17 shows the effect of the training overhead in each updating strategy for the 8-12 system and varying burst length.

Some partial conclusions are:

- ◆ As expected, the performance gets better from strategy “training only” to strategy “reprocess”
- ◆ However, as the burst length and/or training overhead increases the performance gain from the most complex strategy diminishes as compared to simpler ones
- ◆ Architecture 8–12 requires higher SNR for same performance than 4–8 system
- ◆ With higher burst length L and training overhead it is possible to attain a high fraction of the optimal MMSE performance
- ◆ Also with higher burst length L , the effect of increasing the training overhead from 10% to 30% is almost negligible independently of chosen updating strategy.

5. CHANNEL CAPACITY

The capacity of the aforementioned system, for a particular realization of the channel matrix \mathbf{H} is given by [5]:

$$C = \log_2 \det \left[\mathbf{I}_M + \frac{r}{N} \mathbf{H}\mathbf{H}^H \right] \quad (7)$$

in bits/s/Hz, where “det” means the determinant operation and \mathbf{I}_M is the identity matrix of order M . The channel capacity in (7) is actually a random variable due to the random nature of channel matrix \mathbf{H} . In the sequel, we refer to channel capacity as the expected value of (7) when averaged over the possible realizations of \mathbf{H} and assuming perfect knowledge about \mathbf{H} . Finally, notice that channel capacities are given under minimum transmission bandwidth requirements.

Figs. 18 and 19 illustrate channel capacity aspects of theoretical and simulated systems. The expectation of (7) was numerically evaluated and is plotted for the 4-8 and 8-12 cases. In particular, these results are in accordance with [5]. The well-known 1-1 Shannon limit is also plotted for comparison. The spectral efficiencies of the MMSE case for 4-8 and 8-12 systems are clearly indicated.

Other points indicate the achievable spectral efficiencies with practical architectures and varying parameters (burst length, training overhead, updating strategy). These capacity points were extracted directly from figs. 2 to 13 for fixed BERs of 10^{-2} and 10^{-3} . The capacity figures of figs. 18 and 19 indicate opportunities for very high data rates on the wireless channel.

The training overhead is discounted in the capacity calculations for practical schemes. For example, with 20% training overhead, a 8-12 system would offer $8 \times 2 \times 0,80 = 12,8$ b/s/Hz. For the MMSE case we considered 0% training overhead in order to give an insight about the limits of the capacities achievable with linear processing and those particular parameters.

Another interesting comparison can be done with conventional PSK modulation schemes. For example, with 4 transmit antenna and QPSK modulation per transmit antenna, the maximum

spectral efficiency would be 8 b/s/Hz. This is equivalent to a 256-PSK modulation. However, the 256-PSK modulation would require a SNR of approximately 40 dB in an AWGN channel in order to achieve 1% BER (according to eq.(5-2-61) of [6]). According to figs. 1 to 3, with the 4-8 system evaluated in this paper, a similar spectral efficiency can be achieved with a SNR of 10 dB or less.

6. CONCLUSIONS

In this paper we investigated the effects of different receiver adaptive strategy in a multiple transmit-receive antenna wireless link. The results may serve as basis in practical guidance when analyzing the tradeoffs existing between performance and complexity among the different options. The choice of which transmitter-receiver architecture, burst length, training overhead and updating strategy would ultimately be based on the amount of implementation resources available as well as on the desired minimum BER performance.

The paper also gives some illustrative figures about the range of channel capacities potentially achievable with such communications architecture. It clearly signalsizes for opportunities of very high data rates on the wireless channel.

ACKNOWLEDGEMENTS

We would like to thank the valuable discussions with Prof. Elvio Cesar Girauda, from DEE/UFC, specially regarding the topics discussed in section 5.

REFERENCES

- [1] G. J. Foschini, “Layered Space-Time Architecture for Wireless Communications in a Fading Environment when using Multiple Antennas”, Bell Labs Tech. J., v.1, n.2, 1996, pp.41-59.
- [2] G. D. Golden, G.J. Foschini, R.A. Valenzuela, P.W. Wolniansky, “Detection Algorithm and Initial Laboratory Results using the V-BLAST Space-Time Communications Architecture”, Electronics Letters, v.35, n.7, Jan., 1999, pp. 14-15.
- [3] T.L. Marzetta, B.M. Hochwald, “Capacity of a Mobile Multiple-Antenna Communication Link in Rayleigh Flat Fading”, IEEE Trans. Info. Theory, v.45, n.1, Jan. 1999, pp.139-157.
- [4] S .Haykin, *Adaptive Filter Theory*, 3ed., Prentice-Hall, 1996
- [5] G. J. Foschini and M. J. Gans, “On Limits of Wireless Communications in a Fading Environment When Using Multiple Antennas”, Wireless Personal Communications, v. 6, n. 3, March 1998, pp. 311-335.
- [6] J.G. Proakis, *Digital Communications*, 3ed., McGraw-Hill, 1995

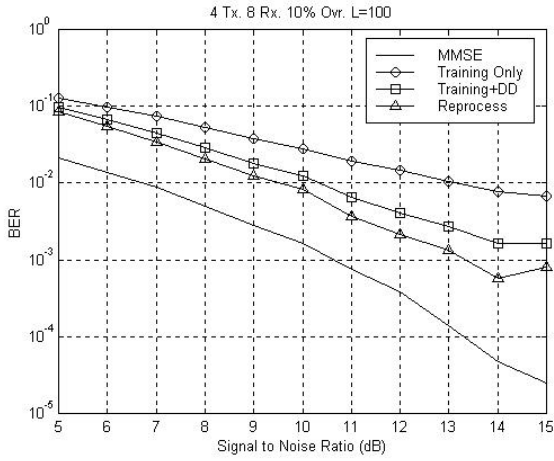


Fig. 2

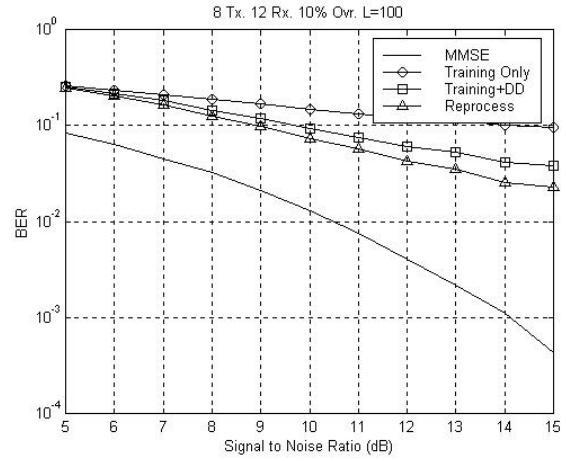


Fig. 5

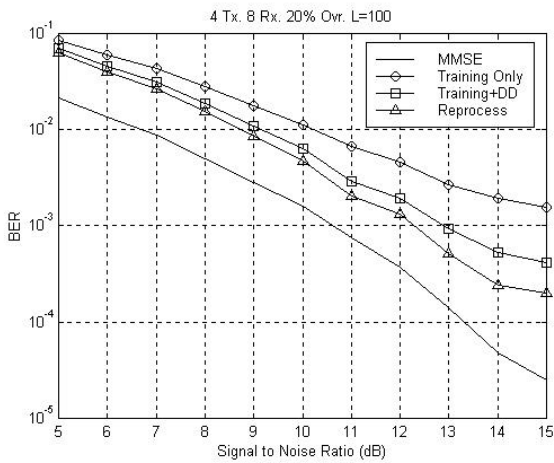


Fig. 3

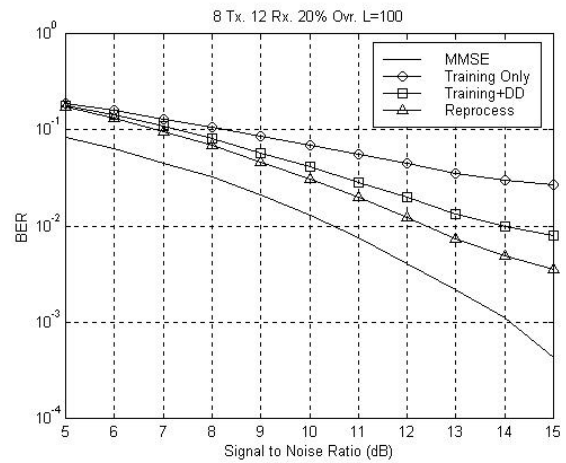


Fig. 6

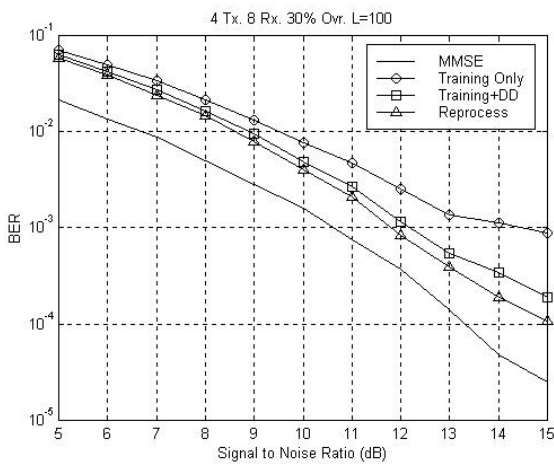


Fig. 4

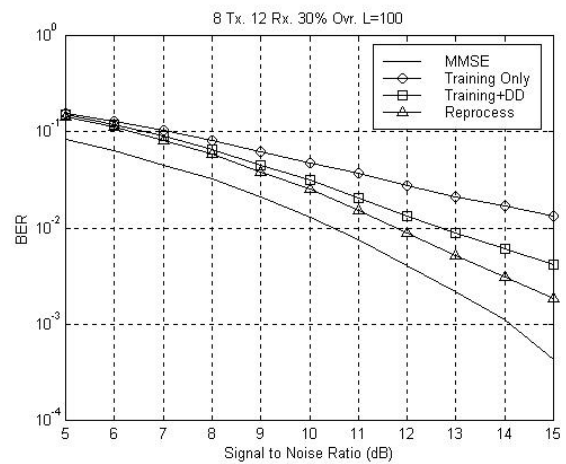


Fig. 7

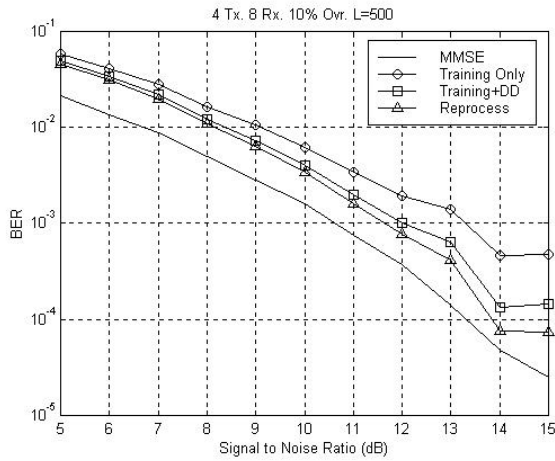


Fig. 8

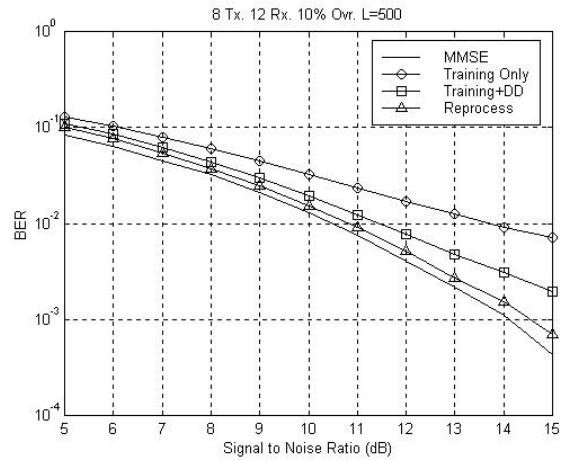


Fig. 11

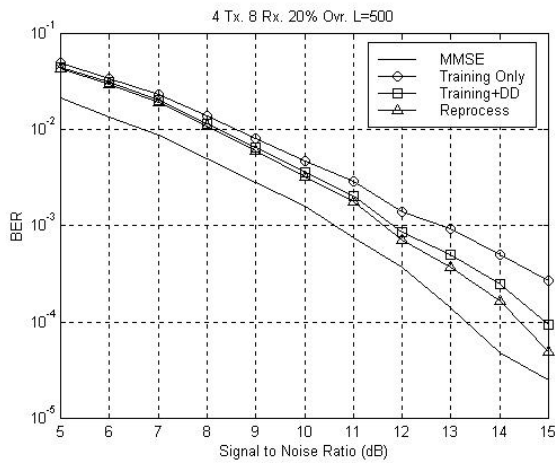


Fig. 9

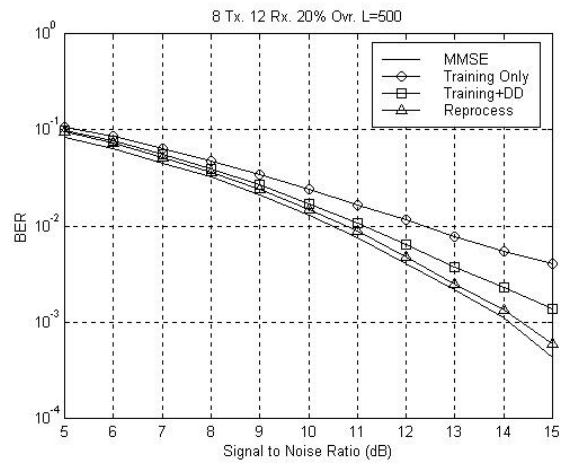


Fig. 12

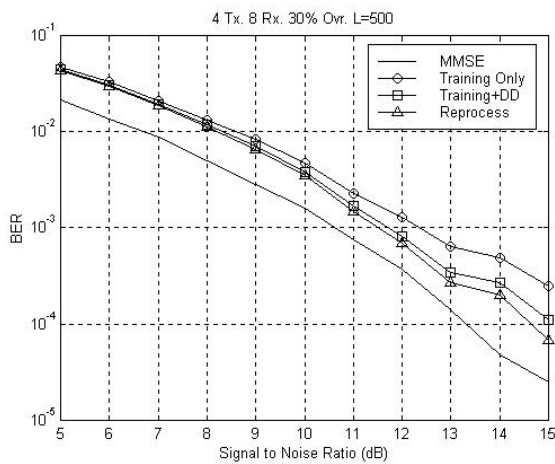


Fig. 10

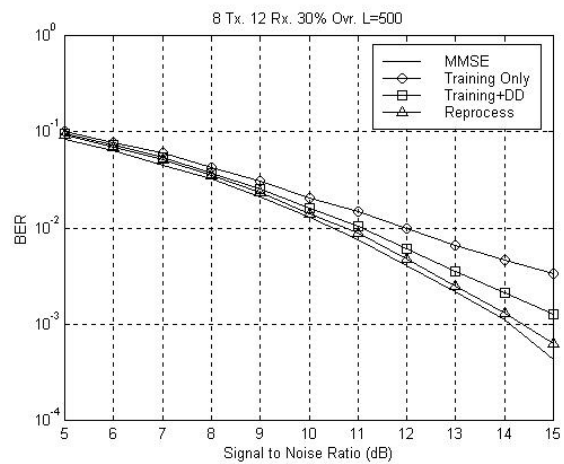


Fig. 13

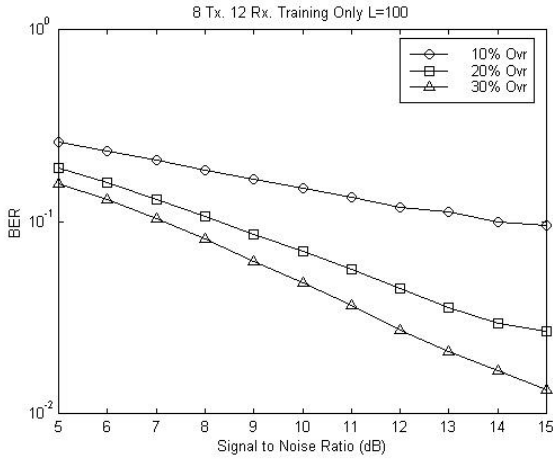


Fig. 14

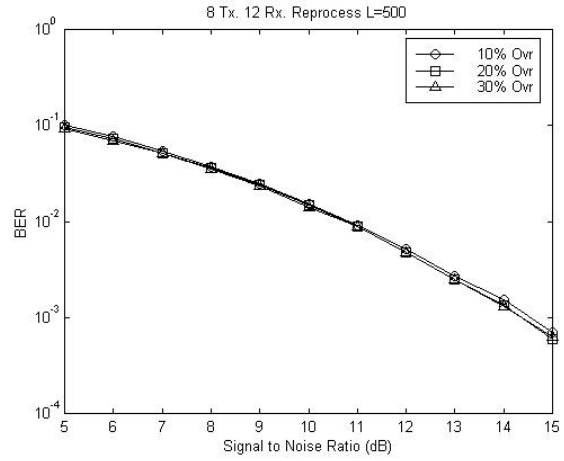


Fig. 17

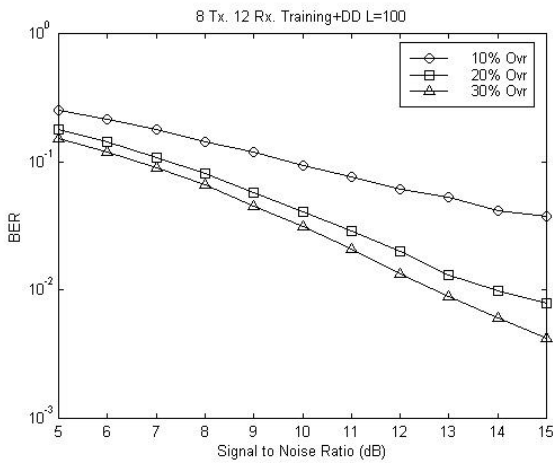


Fig. 15

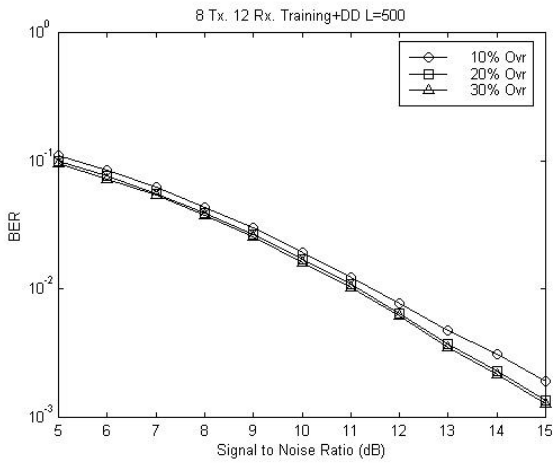


Fig. 16

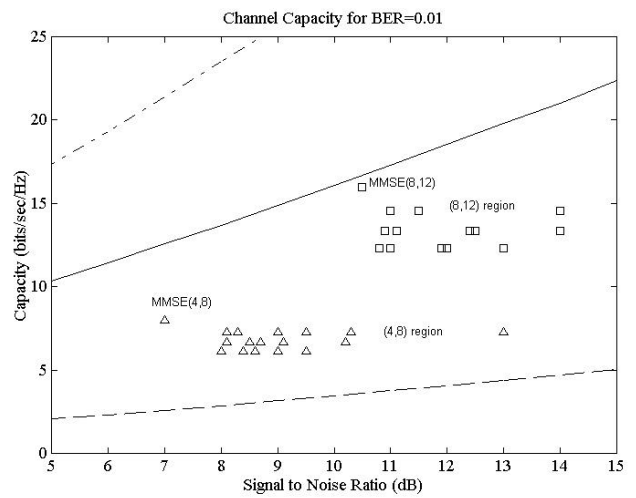


Fig. 18: Theoretical limits: -- 1-1 system, — 4-8, -.- 8-12

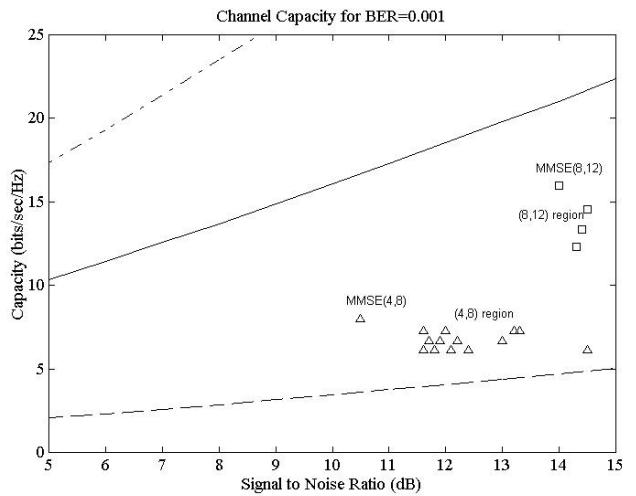


Fig. 19: Theoretical limits: -- 1-1 system, — 4-8, -.- 8-12